Research Article | Vol. 24, No. 25 | 12 Dec 2016 | OPTICS EXPRESS 28669

Optics EXPRESS

Longitudinal iso-phase condition and needle pulses

KEVIN J. PARKER[1,*] AND MIGUEL A. ALONSO[2]

[1]*Department of Electrical and Computer Engineering, University of Rochester, Hopeman Building 203, PO Box 270126, Rochester, NY 14627-0126, USA*
[2]*The Institute of Optics, University of Rochester, Wilmot Building, PO Box 270186, Rochester, NY 14627-0186, USA*
**kevin.parker@rochester.edu*

Abstract: We study the properties of pulsed solutions to the scalar and vector wave equations composed of plane-waves with equal longitudinal spatial frequency. This condition guarantees that, at all times, the field profile is invariant in the longitudinal direction. Particular emphasis is placed on solutions with rotational symmetry. For these solutions, the wave concentrates strongly near the axis at a given time. We provide closed-form expressions for some of these fields, and show that their wavefronts are approximately spherical. Solutions carrying orbital and spin angular momenta are also considered.

OCIS codes: (070.3185) Invariant optical fields; (070.7345) Wave propagation; (350.5500) Propagation; (320.5540) Pulse shaping.

References and links

1. A. E. Siegman, *Lasers* (Univ. Science Books, 1986).
2. M. A. Alonso and N. J. Moore, "Basis exoansions for monochromatic field propagation in free space," in *Mathematical Optics: Classical, Quantum, and Computational Methods*, V. Lakshminarayanan, ed. (CRC Press, 2012), chap. 4, pp. 97–141.
3. J. Durnin, "Exact solutions for nondiffracting beams. I. The scalar theory," J. Opt. Soc. Am. A **4**(4), 651–654 (1987).
4. J. C. Gutiérrez-Vega, M. D. Iturbe-Castillo, and S. Chávez-Cerda, "Alternative formulation for invariant optical fields: Mathieu beams," Opt. Lett. **25**(20), 1493–1495 (2000).
5. C. J. R. Sheppard, "Bessel pulse beams and focus wave modes," J. Opt. Soc. Am. A **18**(10), 2594–2600 (2001).
6. C. J. R. Sheppard, "Generalized Bessel pulse beams," J. Opt. Soc. Am. A **19**(11), 2218–2222 (2002).
7. J. Turunen and A. T. Friberg, "Propagation-invariant optical fields," in *Progress in Optics* vol. 54 E. Wofl, ed. (Elsevier, 2009), pp. 2–85.
8. J.-Y. Lu and J. F. Greenleaf, "Nondiffracting X waves-exact solutions to free-space scalar wave equation and their finite aperture realizations," IEEE Trans. Ultrason. Ferrelec. Freq. Control **39**(1), 19–31 (1992).
9. J. Salo, A. T. Friberg, and M. M. Salomaa, "Orthogonal X waves," J. Phys. A **34**, 7079–7082 (2001).
10. J. W. Goodman, *Introduction to Fourier Optics*, (Roberts & Co., 2005), pp. 31–62.
11. M. Born and E. Wolf, *Principles of Optics* (Pergamon Press, 1980), pp. 556–592.
12. E. G. Williams, *Fourier acoustics: sound radiation and nearfield acoustical holography* (Academic Press, 1999), pp. 1–13.
13. R. N. Bracewell, *The Fourier Transform and its Applications* (McGraw-Hill, 1965), p. 112.
14. M. V. Berry, "Evanescent and real waves in quantum billiards and Gaussian beams," J. Phys. Math. Gen. **27**(11), L391–L398 (1994).
15. C. J. R. Sheppard and S. Saghafi, "Beam modes beyond the paraxial approximation: A scalar treatment," Phys. Rev. A **57**(4), 2971–2979 (1998).
16. M. A. Alonso, "The effect of orbital angular momentum and helicity in the uncertainty-type relations between focal spot size and angular spread," J. Opt. **13**(6), 064016 (2011).
17. J. A. Jensen, "Simulation of advanced ultrasound systems using Field II," in *Biomedical Imaging: Nano to Macro, 2004. IEEE International Symposium on* (2004), pp. 636–639 Vol. 631.
18. J. A. Jensen, "Field: a program for simulating ultrasound systems," in *10th Nordibaltic Conference on Biomedical Imaging*(1996), pp. 351–3553.
19. H. E. Kondakci and A. F. Abouraddy, "Diffraction-free pulsed optical beams via space-time correlations," Opt. Express 24(25), 28659–28668 (2016).

#275968 http://dx.doi.org/10.1364/OE.24.028669
Journal © 2016 Received 15 Sep 2016; revised 5 Nov 2016; accepted 6 Nov 2016; published 2 Dec 2016
Corrected: 5 December 2016

Optics EXPRESS

1. Introduction

The wave and Helmholtz equations cover a wide range of applications in electromagnetics, acoustics, and quantum mechanics. These equations accept a large number of fairly simple closed-form solutions within the paraxial approximation, such as monochromatic and pulsed Gaussian beams and their higher order generalizations [1,2]. Even beyond the paraxial regime, there are several exact monochromatic solutions with interesting properties that have been the subject of much attention. These include not only plane waves but also the so-called Bessel [3] and Mathieu [4] beams. Such solutions are sometimes called "nondiffracting beams" given that their transverse profile is maintained under propagation, However, like other authors, we prefer the adjective "propagation-invariant" over "nondiffracting" as the latter could give the incorrect impression that these solutions bypass a physical law. Similarly, we use the more general noun "field" rather than "beam" since the latter indicates a field that is well collimated and whose transverse power distribution is confined to a finite region at all times.

Polychromatic solutions with interesting behaviors have also been considered, in particular those that can be expressed as a coherent superposition of Bessel fields. As noted by Sheppard [5,6] and Friberg and Turunen [7], there are three types of such solutions that are of particular interest. The first corresponds to superpositions in which the nodal cylindrical surfaces coincide for all frequencies. The second is the superposition of beams with equal cone angle, which gives rise to the well-known X-wave pulses [8,9]. The third type can be generalized to give nondispersive pulses with arbitrary group velocity. The solutions proposed in this work belong to this third class, in the limit of zero group velocity.

A useful approach to analyzing and propagating waves is the angular spectrum [10–12]. In this article we use the angular spectrum to determine the necessary and sufficient conditions for all components of the angular spectrum to propagate forward accumulating equal longitudinal phases. This condition guarantees that the z dependence of the solutions is separable, which implies that at any given time the field is self-similar. We show that, both in two and three dimensions, many closed-form scalar solutions can be found. The simplest of these solutions have wavefronts that most of the time are very close to hemispherical, all with the same (time-dependent) radius of curvature, but longitudinally displaced. At a given time, however, they collapse onto a strongly transversely localized distribution free of the typical Bessel side lobes. These solutions involve finite power (unlike Bessel fields and plane waves) but not finite energy given their infinite longitudinal extent. We discuss how a variety of closed-form versions of these solutions can be found that carry a finite amount of energy, at the cost of the dependence in z not being exactly separable. For simplicity, we start by considering solutions to the scalar wave equation, and then we propose simple generalizations to transverse vector waves that satisfy the free-space Maxwell equations.

2. Theory

2.1 The angular spectrum

The angular spectrum and its use for plane-to-plane propagation can be summarized succinctly: Let $\tilde{p}(x,y,0;\omega)$ be a monochromatic wave scalar quantity in free space with frequency ω. Then, in the plane of $z=0$,

$$\tilde{p}(x,y,0;\omega)=\int_{-\infty}^{+\infty}\int_{-\infty}^{+\infty}\tilde{\boldsymbol{P}}(k_x,k_y,0;\omega)\mathbf{e}^{i(k_x x+k_y y)}dk_x,dk_y \tag{1}$$

and

$$\tilde{\boldsymbol{P}}(k_x,k_y,0;\omega)=\frac{1}{4\pi^2}\iint\tilde{p}(x,y,0;\omega)\mathbf{e}^{i(k_x x+k_y y)}dxdy, \tag{2}$$

Optics EXPRESS

a transverse spatial Fourier transform pair, where k_L^{-1} is the angular spectrum as a function of wavenumber $k = 2\pi/\lambda = \omega/c$ (λ being the wavelength and c the wave speed).

An important feature of the angular spectrum relates to propagation from the plane $\tilde{p}(x, y, 0; \omega)$ to a parallel plane $\tilde{p}(x, y, z; \omega)$: the transfer function relation can be written simply as

$$\tilde{\boldsymbol{P}}(k_x, k_y, z; \omega) = \tilde{\boldsymbol{P}}(k_x, k_y, 0; \omega)\mathbf{e}^{ik_z z} \tag{3}$$

where

$$k_z = \sqrt{k_2 - k_x^2 - k_y^2}. \tag{4}$$

For plane wave propagation in the + z direction one must use the positive real root of Eq. (4) when $k_x^2 + k_y^2 \le k^2$ (propagating waves), and the positive imaginary root when $k_x^2 + k_y^2 > k^2$ (evanescent waves). The solutions we consider in what follows do not involve evanescent components, so the square root is taken as real and positive and the phase of the transfer function is $k_z z = z\sqrt{\omega^2/c^2 - k_x^2 - k_y^2}$. . In the time domain, the field can then be written as

$$p(x, y, z; t) = \int_{+\infty}^{+\infty} \tilde{p}(x, y, z; t)\mathbf{e}^{-i\omega t}\, d\omega = \int_{+\infty}^{+\infty}\int_{+\infty}^{+\infty}\int_{+\infty}^{+\infty} \tilde{\boldsymbol{P}}(k_x, k_y, 0; \omega)\mathbf{e}^{i(k_x x + k_y y + k_z z - \omega t)}\, dk_x dk_y d\omega. \tag{5}$$

2.2 The longitudinal iso-phase condition

The longitudinal iso-phase condition corresponds to solutions in which the dependence in the propagation distance z is separable, that is, for which k_z is fixed. For example, for monochromatic beams, this condition reduces to:

$$k_x^2 + k_y^2 = \left(\frac{\omega}{c}\right)^2. \tag{6}$$

In circularly symmetric beams this leads to the Bessel field solution [3]. However, in this work we consider broadband excitations, so the iso-phase condition restricts combinations of ω, k_x , k_y for which

$$k_z^2 = \left(\frac{\omega}{c}\right)^2 - k_x^2 - k_y^2 = k_L^2, \tag{7}$$

where $k_L > 0$ is constant. Note that the factorization of the dependence in z as a simple exponential means that the pulse has vanishing group velocity [7]: the intensity profile of the solutions evolve in time and in the transverse dimensions, but not in the main direction of propagation despite the wave being composed only of forward propagating traveling waves.

2.3 Solutions in two dimensions

We now examine the simplest case of two-dimensional propagation, where the source is distributed along a line. This starting point has a few beneficial features. Many practical applications in acoustics, medical ultrasound, and radar use 1D arrays that are well-suited to the simpler solution. Two-dimensional (2D) arrays are also commonly excited using separable, orthogonal, 1D functions. Finally, the 2D solution has properties that are easy to visualize and appreciate.

In 2D, the longitudinal iso-phase condition reduces to:

Optics EXPRESS

$$\left(\frac{\omega}{c}\right)^2 - k_x^2 = k_L^2. \tag{8}$$

Let us choose a lowest, or base frequency ω_L, defined as a plane wave in the z-direction, so

$$k_L^2 = \left(\frac{\omega_L}{c}\right)^2. \tag{9}$$

All higher frequencies $\omega \geq \omega_L$ can meet the longitudinal iso-phase condition. In a dispersion-free medium such as free space where $c(\omega) = c_0$:

$$k_x^2 = \frac{1}{c_0^2}(\omega^2 - \omega_L^2). \tag{10}$$

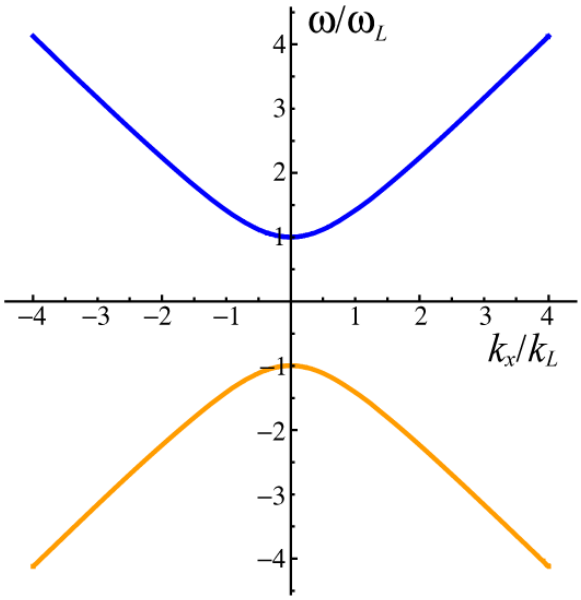

Fig. 1. Hyperbola in the 2D Fourier plane defining the iso-phase condition. For forward-propagating fields and when the analytic signal representation is used only the top (blue) branch is used.

This defines a hyperbola in the 2D Fourier space of $[k_x, \omega]$, as shown in Fig. 1. This hyperbola has two branches, corresponding to positive and negative temporal frequencies. We choose to use the analytic signal representation of the field, so we only use the positive frequency branch whose vertex is at $[0, \omega_L]$; the real field results from using the real part of the solution.

Accordingly, we seek to create in the plane $z = 0$ the scalar function characterized by the angular spectrum

$$\tilde{\boldsymbol{P}}(k_x, 0; \omega) = A(k_x)\delta\left[k_x^2 - \frac{1}{c_0^2}(\omega^2 - \omega_L^2)\right], \quad \omega \geq 0, \tag{11}$$

Optics EXPRESS

where $\delta[\cdot]$ is the two-dimensional Dirac unit impulse function [13] and an apodization function $A(k_x)$ is included as a practical matter for limited power. The field then yields

$$p(x,z;t)=\mathbf{e}^{ik_L z}\int_{k=-\infty}^{+\infty}\int_{\omega=0}^{+\infty}A(k_x)\delta\left[k_x^2-\frac{1}{c_0^2}(\omega^2-\omega_L^2)\right]\mathbf{e}^{i(k_x x-\omega t)}d\omega dk_x. \tag{12}$$

Integrating first over ω yields

$$p(x,z;t)=\mathbf{e}^{ik_L z}\int_{-\infty}^{\infty}\frac{A(k_x)}{\sqrt{k_x^2+k_L^2}}\exp\left[i\left(k_x x-c_0 t\sqrt{k_x^2+k_L^2}\right)\right]dk_x. \tag{13}$$

Note that this integral can be rewritten by parametrizing $k_x=k_L\sinh\eta$ leading to

$$p(x,z;t)=c_0\mathbf{e}^{ik_L z}\int_{-\infty}^{\infty}A(k_L\sinh\eta)\exp\left[ik_L(x\sinh\eta-c_0 t\cosh\eta)\right]d\eta. \tag{14}$$

The case for which A is chosen to be constant leads to a closed-form solution in terms of modified (or hyperbolic) Bessel functions [13]. Given its infinite power, however, such a solution is singular. There are also important details in the choice of the branches of the square roots that enter that solution depending on the values of x and t. Both these issues can be addressed by considering instead a finite-power solution corresponding to the apodization

$$A(k_L\sinh\eta)=\exp\left[-k_L c_0 q\cosh\eta\right], \tag{15}$$

where q is a positive constant. From the substitution of Eq. (15) into Eq. (14) it can be seen that this is equivalent to shifting the origin in time t by an imaginary amount to $t - iq$. This apodization through a complex displacement of a variable is analogous to those used in the space domain to achieve nonparaxial analogs of Gaussian beams [14,15]. The solution to the integral is found to be given in the compact form

$$p(x,z,t)=\frac{c_0}{2}K_0\left[k_L\sqrt{x^2-c_0^2(t-iq)^2}\right]\exp(ik_L z), \tag{16}$$

where K_0 is a modified Bessel function of the second kind of order 0, and the branch cut of the square root is assumed at the negative real axis of its argument. The fact that the solution is a modified Bessel function can be understood easily. Firstly, assuming that the field is separable as $p(x,z;t)=f(x;t)\exp(ik_L z)$ and substituting it into the wave equation leads to a hyperbolic equation for f that is mathematically analogous to the (1 + 1)D Klein-Gordon equation for relativistic quantum mechanics. By then using an ansatz $f(x;t)=g(\rho)$ with $\rho=\sqrt{x^2-c_0^2(t-iq)^2}$ one finds that g satisfies the modified Bessel differential equation.

To generate this field, the broadband source distribution at plane $z = 0$ is simply the real part of Eq. (17) with $z = 0$. For 1D arrays in ultrasound applications, spatial samples of this real part would constitute the source excitation signals, typically voltages applied to the individual sub-wavelength elements of the 1D array. Note that $t = 0$ does not correspond to the initial time but to the time at which the field is most concentrated spatially; in theory the excitation must exist for all negative times. The parameter q determines the width of the spectrum used, and therefore how thin the field becomes at $t = 0$. Several cases are shown in Fig. 2, corresponding to different values of q. The corresponding fields at different times are shown in the left column in Fig. 3 and Visualization 1 for $k_L c_0 q=1$. We can see from those figures that the transverse width of the field scales with time roughly as $2\sqrt{c_0^2 t^2+q^2}$, so for t

Optics EXPRESS

= 0 the field collapses into a needle-like thin power distribution with no side lobes. We therefore refer to these solutions as "needle pulses".

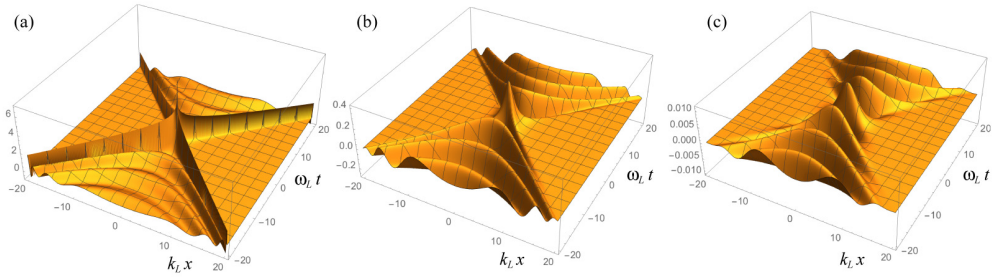

Fig. 2. Excitation signal at the initial plane, for $k_L c_0 q$ = 0.001 (a), 1 (b), and 4 (c).

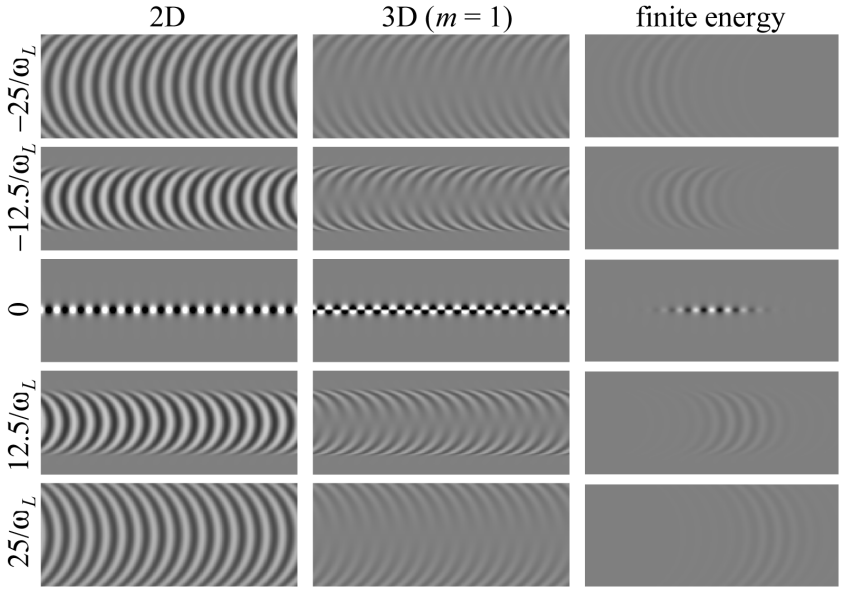

Fig. 3. Real part of the pulses for (left) two dimensions given in Eq. (16), (middle) three dimensions with unit vorticity, and (right) the three-dimensional pulses in Eq. (21), at five different times. For the first two columns, $x \in [-20/k_L, 20/k_L]$ (vertical) and $z \in [0,100/k_L]$ (horizontal), while for the third, $x \in [-20/K_L, 20/K_L]$ and $z \in [-50/K_L, 50/K_L]$.

Note from Fig. 3 that the wavefronts are approximately circular. This can be understood by using the fact that $K_0(i\tau)$ is proportional to a Hankel function of τ. By using the fact that a Hankel function is approximately proportional to the exponential of i times its argument, one finds that the wavefronts are defined by the approximate form, for $t^2 >> q^2$:

$$x^2 + (z - z_0)^2 \approx c_0^2 (t^2 - q^2), \tag{17}$$

where z_0 is a constant that determines the wavefront in question.

The solutions given earlier are of course not the only ones of their type. In fact, since the Laplacian and second time derivative operators that appear in the wave equation commute with derivatives in x or t, any combination of transverse or temporal derivatives of these solutions are also solutions. Combinations of derivatives in x can be used, for example, to create fields with nodal lines.

Optics EXPRESS

2.4 Solutions in three dimensions with rotational symmetry

Analogous results can be found for fields in three dimensions. For example, the following finite-power solution exists which has rotational symmetry:

$$p(\rho,z,t)=c_0\frac{\exp\left[-k_L\sqrt{\rho^2-c_0^2(t-iq)^2}\right]}{k_L\sqrt{\rho^2-c_0^2(t-iq)^2}}\exp(ik_Lz), \tag{18}$$

where $\rho=\sqrt{x^2+y^2}$. By using the same arguments as in the previous section, it is easy to show that these solutions have approximately spherical wavefronts, that they also have a full width of approximately $2\sqrt{c_0^2t^2+q^2}$, and that the parameter q regulates how spatially localized these solutions are at $t = 0$. Further, by applying appropriate operators [16] one can find other interesting solutions. For example, applying m times the vorticity ladder operator $\hat{C}_\pm=\mathbf{v}_\pm\cdot\nabla$ (where $\mathbf{v}_\pm=(1,\pm i,0)/\sqrt{2}$) to the solutions above gives rise to closed-form expressions for fields with vorticity $\pm m$, so that the needle at $t = 0$ is hollow. The right column of Fig. 3 and Visualization 2 show longitudinal cross sections of the real part of such fields with unit vorticity and $k_Lc_0q=1$.

Further, if solutions not to the scalar wave equa z_0 tion but to the free-space Maxwell equations are desired, one can apply vector operators to $\mathbf{v}_\pm=(1,\pm i,0)/\sqrt{2}$ the scalar solutions. For example, the following operator transforms a scalar solution into a similar transverse vector solution with definite helicity (that is, whose monochromatic plane wave components have circular polarization):

$$\hat{\mathbf{C}}_\pm p=\frac{1}{2}\left[(\mathbf{v}_\pm\cdot\nabla)\nabla\pm i\frac{\mathbf{v}_\pm\times\nabla}{c_0}\frac{\partial}{\partial t}-\frac{\mathbf{v}_\pm}{c_0^2}\frac{\partial^2}{\partial t^2}\right]p. \tag{19}$$

Linear combinations of the form $\left[\exp(i\alpha/2)\hat{\mathbf{C}}_+ + \exp(-i\alpha/2)\hat{\mathbf{C}}_-\right]p$, where α is real, lead to pulses that have approximately linear polarization at $t = 0$, with an orientation determined by α. Finally, azimuthal and radial polarizations can be achieved through the action of the following operators, where $\mathbf{z} = (0,0,1)$:

$$\hat{\mathbf{C}}_\mathrm{A}p=(\mathbf{z}\times\nabla)p,\qquad \hat{\mathbf{C}}_\mathrm{R}p=\nabla\times(\mathbf{z}\times\nabla)p. \tag{20}$$

In all cases, an appropriate constant factor must also be used for unit correction.

2.5 Needle pulses with limited energy

k_L The apodization function used earlier means that the fields do not require an infinite amount of power. They do require in theory an infinite amount of energy, since they exist for all time and extend indefinitely in the z direction. In is therefore interesting to consider pulsed versions of these fields that have also finite energy. This is particularly easy to achieve with the three-dimensional pulses in Eq. (18), whose k_L^{-1} depende k_L nce in is simply as a linear factor in the exponent and a global factor of . One can find closed-form finite-energy solutions simply by integrating in the product of Eq. (18) with k_L and a weight function of k_L centered around a longitudinal wavenumber K_L and whose inverse Fourier transform can be found analytically:

$$p_2(\rho,z,t)=\int_{-\infty}^{\infty}k_Lp(\rho,z,t)F(k_L-K_L)dk_L=p(\rho,z,t)\big|_{k_L=K_L}f\left(z+i\sqrt{\rho^2-c_0^2(t-iq)^2}\right), \tag{21}$$

Optics EXPRESS

where $F(k_z)$ is the Fourier transform of . That is, the finite-energy solution is just the product of the infinite-energy solution times an envelope analytic function of a complex argument. For example, using a Gaussian weight of width δ gives

$$\begin{aligned} p_2(\rho,z,t) &= \int_{-\infty}^{\infty} k_L p(\rho,z,t) \frac{1}{\sqrt{2\pi}\delta} \exp\left[-\frac{(k_L-K_L)^2}{2\delta^2}\right] dk_L \\ &= p(\rho,z,t)\big|_{k_L=K_L} \exp\left[-\frac{\delta^2}{2}\left(z+i\sqrt{\rho^2-c_0^2(t-iq)^2}\right)^2\right], \end{aligned} \tag{22}$$

The third column of Fig. 3 and Visualization 3 show this pulse at five different times for $\bar{\omega}_L q = 1$ and $\delta = K_L/10$. Strictly speaking, this solution includes a small amount of backward propagating components, since the Gaussian tails extend over all negative values of k_L. One could limit the integration region to the positive semi-axis (giving a solution for *f* in terms of error functions), or use other options for *F* that vanish explicitly for $k_L < 0$ such as rectangle or semicircle functions or the product of Heaviside step functions and decaying exponentials.

2.6 Ultrasound linear array results

The longitudinal iso-phase solution is applicable to the field of ultrasound since acoustic waves are solutions to the scalar wave equation, and dispersion in water-based materials is negligible. As an independent test of these solutions, relevant to the domain of medical ultrasound imaging using one dimensional linear arrays, the excitation function shown in Fig. 4(a) was applied in the Field II simulation program [17, 18] to a 5 Mhz 100% bandwidth array of the class commonly used in clinical scanners. Specifically, ω_L was set to 5.0 MHz, and the excitation function was sampled in time at 500 Mhz and sampled in the spatial dimension at increments of 0.0495 mm commensurate with the pitch of the elements of the linear array. To apply strict limits on time and space, a Gaussian apodization function was multiplied to the excitation function of Fig. 4(a), with 6σ in time of 6 microseconds and 6σ in space of 256 active transducer elements (13 mm). For convenience, the speed of sound c was set to 1000 m/sec.

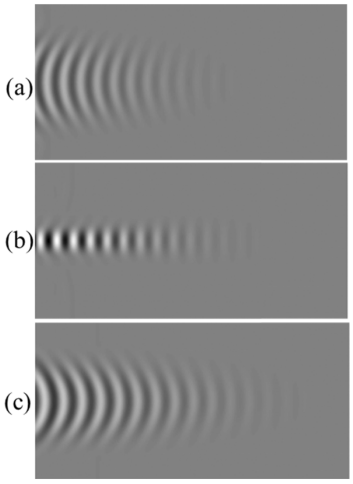

Fig. 4. 5Mhz medical ultrasound linear array simulation of the acoustic pressure field resulting from the longitudinal iso-phase excitation with additional Gaussian apodization in time and space. Three time points are shown, before and after the convergence of the broadband components at time steps proportional to $2\pi/\omega_L$. Image size (vertical or transverse dimension x horizontal or axial dimension): 1.55mm x 3.75mm.

Optics EXPRESS

The simulated ultrasound field demonstrates the principal characteristics of the solutions shown in Fig. 3, in that they exhibit spherical curvature over an extended axial range, then a convergence followed by a reverse spherical curvature. The axial extent is seen to be limited by the aggressive time and space apodization applied at the source plane.

3. Discussion

We found broadband fields whose dependence in the longitudinal direction is separable from that in the transverse ones as well as from time. Surprisingly, there are simple closed form solutions with controllable localization factors, both in two and three dimensions, for scalar and electromagnetic fields. For the scalar solutions with rotational symmetry discussed here, the wavefronts are approximately a train of identical hemispherical shells whose radius varies with time. At the time of maximal focusing, these fields take the form of long, needle-like distributions of optical (or acoustic) power.

Considering implementation in optical systems, it is interesting to note that the longitudinal iso-phase condition is reminiscent of the dispersion relation for a slab metallic waveguide filled with a material with negligible dispersion, except that the role of the transverse and longitudinal directions are reversed. This suggests one mechanism for generating this type of field: a broadband coherent focused pulse can be made to pass through a thin, high-Q, Fabry-Perot planar cavity with negligible material dispersion. The cavity would transmit only plane wave components in different directions that approximately satisfy the longitudinal iso-phase condition. In ultrasound, sonar, and radar applications, on the other hand, these pulses can be generated simply by appropriate phasing of the source array elements.

As these results are preliminary, further work is required to make detailed comparisons of these needle pulse fields against other commonly used pulses with some form of propagation invariance. In particular, we recently learned that another group has been studying similar pulses and that their work will appear published concurrently with ours [19]. The potential applications are quite broad, ranging from imaging in pulse-echo systems, to use in conjunction with nonlinear systems and media where the long axis peak spatial and temporal intensity can provide a unique configuration of higher order or supra-threshold effects. However, the relative simplicity of the longitudinal iso-phase condition and the closed-form solutions provides a straightforward means for obtaining further experimental, analytical, and simulation results.

Funding

National Science Foundation (NSF) (PHY-1507278).

Acknowledgments

KJP acknowledges support by the Hajim School of Engineering and Applied Sciences at the University of Rochester and the expert skills in Field II simulations provided by Ph.D. student Shujie Chen.